From Disks to Hexagons and Beyond: A Study in Two Dimensions

Jean-Marc Flesselles, Marcelo O. Magnasco, and Albert Libchaber
The James Franck and Enrico Fermi Institutes, The University of Chicago, 5640 South Ellis Avenue, Chicago, Illinois 60637
(Received 22 July 1991)

Crystallization of two-dimensional domains in monolayer films of the soluble surfactant sodium dodecyl sulfate exhibits a smooth shape transition from disks to hexagons. This transition is experimentally proven to be mainly a kinetic effect. The appearance of negative curvature marks the onset of shape instabilities. A simple geometric model based on the local interplay between line tension and crystalline anisotropy accounts for the observed behaviors. It is argued that the observed shapes are generic and insensitive to details of the actual mechanisms.

PACS numbers: 61.50.Cj, 64.80.−v, 82.65.−i

Theoretical models for two-dimensional growth can be fairly simple [1,2]. An experimental test ground for them is provided by monolayers at the air-water interface [3], as observed by fluorescence microscopy [4,5]. Most studies have concentrated on equilibrium, or quasiequilibrium shapes. Theories have given a satisfactory explanation for some of the observed transitions [6]. In a previous experiment, a solid-liquid transition in the surface monolayer of a solution of sodium dodecyl sulfate (SDS) was reported [7]. It was shown there that faceted growth can occur during solidification. Note that this phenomenon had already been observed in other contexts [8].

In this paper we report an experimental study and a modeling of the transition between rounded and faceted shapes. We focus on the narrow concentration region of the phase diagram where both shapes are observed. We show that this faceting is a kinetic effect and that shapes with positive curvature scale during growth, whereas the appearance of negative curvature marks the onset of instabilities. Then, filaments of different forms start growing from the corners. The onset of instability is triggered by a sufficiently rapid cooling down. We present a simple geometric model based on minimal assumptions. Qualitative understanding of the equation and computer simulations account for the observed experimental behavior: a smooth kinetically induced shape transition, a scaling growth for shapes with positive curvature, destabilization when negative curvature develops.

SDS is a common soluble surfactant. As such, the amount of molecules at the surface is fixed by the chemical potential equilibrium between the surface and the bulk. A solid-liquid transition around room temperature for SDS solutions below the critical micelle concentration has recently been observed by fluorescence microscopy and confirmed by surface tension measurements. Other existing data also seem to exhibit this transition, though it had not been noticed before ([9], see Fig. 1).

SDS purchased from Fluka (better than 99% pure) was dissolved in a 10^{-3}-mol/l solution of NaCl in purified water (pH$\sim$5.5–6, resistivity higher than 10 mΩ cm), in bulk concentration c ranging from 0.015% to 0.20% by weight (0.52×10^{-3} to 6.9×10^{-3} mol/l), hence below the measured critical micelle concentration of 7.7×10^{-3} mol/l (0.22% by weight) at 23 °C. SDS is unstable and undergoes a spontaneous hydrolysis into 1-dodecanol, a strongly insoluble surfactant. We therefore worked as quickly as possible so that results remain reproducible. We observed that within 6 to 10 h, a given film would have a reproducible behavior.

The essential features of our experiment relied on temperature stability. The setup consisted of a square Teflon trough (3.5 cm×3.5 cm), whose bottom was a 50-μm-thick Teflon sheet, screwed to a copper plate in contact with a Peltier element, itself in contact with a thermostated brass plate. A programmable temperature regulation allowed us to work between −5 and 40 °C and to perform quenches or ramps at cooling rates between 0.1 and 100 mK/s with a stability of 1 mK during slow ramps and 4 mK during steady states. A heating glass cover slip closed the cell to protect it from dust contamination and to avoid water condensation. The setup was thermally in-

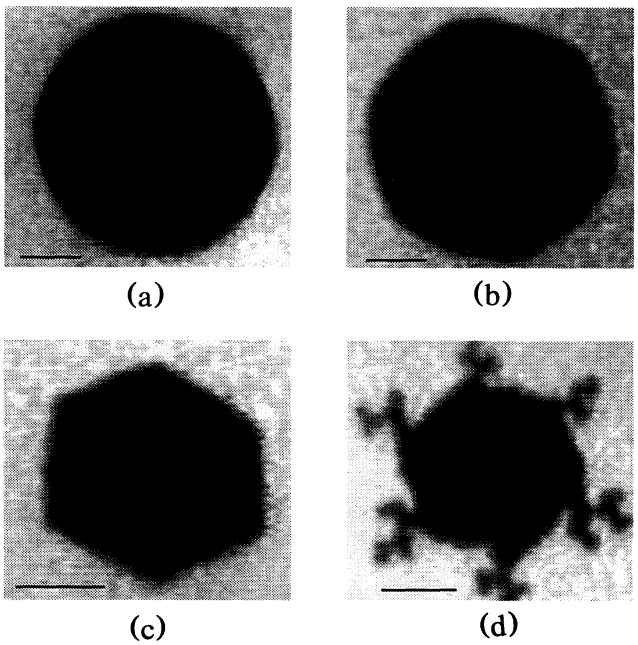

FIG. 1. Growth shapes for different cooling rates. (a) 0.1 mK/s; (b) 5 mK/s; (c) 50 mK/s; (d) 100 mK/s. Note the onset of destabilization into zigzags. Each bar is 10 μm long.

sulated and was placed on a modified microscope stage.

The excitation for fluorescence was provided by the 488-nm line of an Ar laser shining obliquely to the cell, from above. The fluorescence emitted by the probes was cut from the blue light of the laser by a yellow filter inserted in the microscope. Lenses along the light path permitted us to adjust the size of the illuminated spot. Images from a high-sensitivity silicon-intensified-target video camera installed on the microscope were recorded on tapes for later analysis. Spatial resolution was 1 μm. Measurements of the surface temperature with a thermistor showed the cell's response time to be about 100 s.

About 3 ml of fresh solution were pipetted into the trough, after it had been cleaned and rinsed, first with water, then with the solution under study. Most experiments have been conducted with 0.25 μl of BODIPY hexadecanoic acid (from Molecular Probes) as the fluorescent dye, diluted to 10^{-4} mol/l in a 3:1 chloroform/methanol solution. We preferred it because of its low solubility, high brightness, and low bleaching: A laser output power of 5 mW was sufficient during several hours.

During a typical run, the SDS solution and the dye were deposited at 30 °C and left for about 5 min to reach thermal equilibrium. The system was then quenched down to 0 °C and left for about 15 min to ensure a proper chemical equilibrium between bulk and surface. The temperature was then slowly raised until the surface returned to the homogeneous low-density phase. During this ramp, the melting temperature was recorded within 1 °C. Surface flows on the order of 5 to 10 μm/s usually accompanied nucleation and melting, more or less independently of the cooling rate.

Within the appropriate concentration range (0.055–0.060 wt.%), fast rates induce faceting, whereas slow ones favor roughening, the transition from one to the other being smooth. This scenario is systematic and qualitatively reproducible, but the meanings of "fast" and "slow" depend on the actual film, and are probably highly sensitive to the concentration. Typically, fast is above 100 mK/s and slow below 1 mK/s.

We present here representative results obtained on a single film (with SDS bulk concentration $c=0.06$ wt.% and 10^{-3} mol/l NaCl) where ramps at five different cooling rates have been performed: 0.1, 1, 5, 50, and 100 mK/s. The film was systematically raised up to 26 °C at least and left for a couple of minutes until thermal equilibrium. Observed shapes are displayed in Fig. 1. Patterns obtained during the slowest ramp (0.1 mK/s) were nearly perfect disks. At 1 mK/s a sixfold anisotropy was present, though the boundary was smooth all around the edges. At 5 mK/s, the hexagonal symmetry was obvious: The curvature started to concentrate at the corners, whereas the sides flattened out. Nearly perfect hexagons with straight edges occurred at 50 mK/s, whereas the hexagons showed a small outward (negative) curvature at 100 mK/s.

For each of these ramps, we have followed the growth of a single domain since its nucleation. A plot of their areas versus time is presented in Fig. 2. At the higher cooling rates (5, 50, and 100 mK/s), where the shapes are essentially faceted, the growth is roughly linear in time, the rate being about 6 $\mu m^2/s$. At the lower cooling rates (0.1 and 1 mK/s), the variation follows a square law: Incoming matter is homogeneously sticking along the boundary of the domain. The linear law means that the amount of matter added to the growing domain is independent of its size. Thus matter only arrives at some special points on the boundary, which can only be the corners.

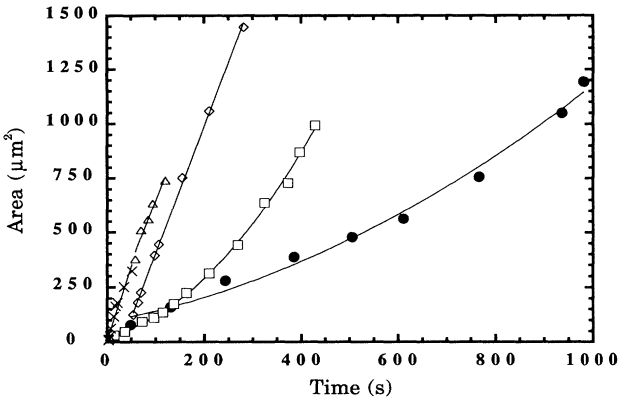

FIG. 2. Variation of the area of domains grown at different cooling rates on a single film (●, 0.1 mK/s; □, 1 mK/s; ◇, 5 mK/s; △, 50 mK/s; ×, 100 mK/s). Errors in the areas are of 10%.

We also have evidence that a similar shape transformation is to be expected as the concentration is varied at a fixed cooling rate. If an SDS solution gave rounded hexagons at the highest possible cooling rate, diluting it would allow it to recover sharper shapes. Our conclusions are as follows: Hexagonal or circular shapes could be obtained whatever the SDS bulk concentration, the faceting being a purely dynamical process. But the experimental time window and the cell's response time limit the observability to a narrow concentration range.

The hexagonal shape can be kept stable if the ramp is properly controlled. Domains as large as 100 μm in diameter have been grown. If the ramp is fast enough, the shape becomes unstable: protrusions of different kinds start growing from the corners leading to a variety of final patterns. In the "subcritical regime," i.e., during growth until the onset of destabilization, hexagons as well as more rounded shapes grow in a scaling fashion. The onset of the instability is marked by the appearance of negative curvature close to the corners: growth continues either by canceling off this curvature or by destabilizing. The hexagonal core of the domain then grows at a much smaller rate, whereas nearly all the matter is added to the corners, enhancing locally the negative curvature. If the domain is small enough, the negative curvature extends

over the whole edge. A limiting shape of small domains before destabilization is close to a star of David (cf. Fig. 3).

Our observations show that the cooling rate induces the destabilization. To differentiate among the other possible parameters, we submitted the film to temperature oscillations once the nucleation had occurred. Both the rate and the amplitude could be tuned independently.

We report here on results obtained on a given film (0.055 wt.% SDS, 10^{-3} mol/l NaCl). The oscillations were performed from the nucleation temperature (observed between 20 and 22 °C) down to 15 °C at 1- and 10-mK/s ramps and down to 5 °C at 100-mK/s ramps. Whereas no destabilization occurred during the slow ramps, the domains destabilized during the fastest one. If a ramp that gave birth to faceted domains was stopped, these domains relaxed to round shapes after about 2 h. These two observations support our conclusion that the cooling rate is the driving parameter, for all shape transformations, and that the absolute undercooling only changes time scales, as one could expect from the constant volume-controlled temperature situation in which the experiment is performed. Since destabilization has been observed on hexagons of sizes over 1 order of magnitude, there is no critical size involved.

Three different patterns arise as the instability develops, which can be classified according to their growth speed. Slow filaments (about 0.3 μm/s) undergo systematic and regular tip splitting at 120° creating regular zigzag patterns [Fig. 1(d)]. Fast growing ones ($\sim$10 μm/s) are thin and straight. They might bend but do not branch and can be several hundreds of microns long. At intermediate speeds ($\sim$1 μm/s) filaments are straight and experience a few branches, usually at about 60° from the growth axis, or tip split in two straight branches at 120° from each other. They are about 100 μm long at most.

Since a quantitative study of the sensitivity to the SDS and the NaCl concentrations has not been done, the results presented in this paper remain essentially qualitative. Our purpose is to describe the relevant features of this transition. The understanding of the underlying microscopic processes is still lacking.

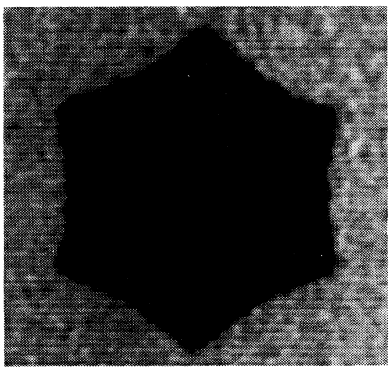

FIG. 3. Typical shape at the onset of destabilization. The waviness at the ridges of the star are due to discretization and imaging artifacts.

A minimal model has to exhibit faceting when the system is driven out of equilibrium and permit a relaxation to the equilibrium shape otherwise. We will now argue that the basic subcritical phenomenology of this system can be explained through simple interface motion equations involving only local interactions. Our first assumption will be that the boundary dynamics can be approximated as "creeping motion" minimizing the interface length [10]. Such an equation can be written as

$$u_\perp = -v(\kappa - 2\pi/L) + \text{sources} \quad (1)$$

(where $u_\perp$ is the outward normal velocity of the boundary, v is a diffusion constant, κ is the curvature, and L is the length of the interface). In the absence of sources, this is a geometric diffusion equation for curvature, preserving the area of the domain through the $2\pi/L$ Lagrange multiplier. Hence the relaxed shape is circular.

The second assumption concerns the sources term. Some preliminary evidence would indicate that the experimental domains are single crystals. We should therefore expect fast and slow directions for crystalline growth. This breaking of orientational symmetry can give rise to dramatic changes in the morphology of a growth model [11]; we will accordingly assume that the sources term depends on the angle θ between the normal to the boundary and some crystallographic axis. There are several ways in which such a term could be constructed and argued for; we will use

$$\text{sources} = R|\kappa|f(\theta), \quad (2)$$

where $\int f(\theta)d\theta = 1$ and $P \equiv R/v$ is the Péclet number, the physical parameter. P equals the rate of matter advection over the diffusion constant along the interface. With this matter term the equation supports scaling solutions; the time derivative of the area is constant and equals Pv, as long as the shape is convex. We have chosen this particular form because it reproduces the phenomenology we have seen and because it makes life easy; we have no stronger evidence in its favor.

If $f(\theta)$ is a set of six Dirac delta functions, the equation has analytically solvable solutions: hexagonlike shapes, whose walls are circular arcs, meeting at the corners; the discontinuity in the normal angle equals $P/6$. When $P = 2\pi$ the solution is a straightsided hexagon. As P increases, the last stable solution is $P = 4\pi$ (a star of David).

A more plausible form for $f(\theta)$ is $\sin^2(3\theta)/\pi$. We have studied it numerically, with a spectrally accurate method. We have found again a set of stable scaling shapes, shown in Fig. 4. For $P = 2\pi$, again the regular hexagon is a stable scaling solution. For $P > 2\pi$, we have stable concave-shaped hexagons. But not for long: At

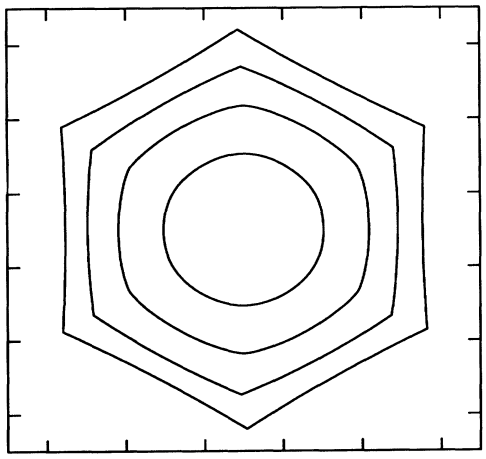

FIG. 4. Stable scaling shapes as a function of P. $P=1$ (innermost), 3,5,7 (outermost).

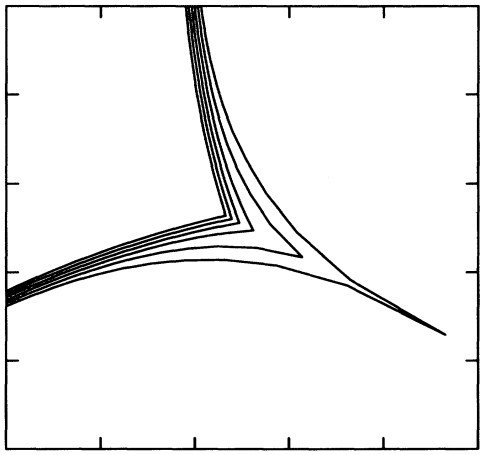

FIG. 5. Destabilization of the tips occurs when P is larger than a critical value. Different curves here present the time evolution of the boundary at $P=8.2$. Outer curves are later times. The numerics lose accuracy after the last shape shown.

$P=8.05\pm0.1$ the system suffers an instability, and the tips begin to grow, quite fast, into filaments, while scarcely any matter is aggregated into the body of the hexagon, as shown in Fig. 5. The precise behavior of the tips should be studied with a subtler implementation of our numerics; the model equation itself, however, will probably suffer some disease. For instance, a huge amount of matter is being added at the narrow, fast-moving tips. Temperature diffusion effects from the release of latent heat should become important. We expect this and other kinetic effects to play a crucial role in the understanding of the supracritical morphology.

This work was initiated by Bruno Berge. He and Adam Simon provided the essential expertise. We wish to thank Haim Izrael and Luc Faucheux for their experimental help, and Steve Langer for discussions. J.-M.F. was supported by a Lavoisier Grant from the French Ministry for Foreign Affairs; M.O.M. acknowledges receipt of a Bloomenthal fellowship. This work was supported by the NSF under Grants No. DMR87-22714, No. DMR88-15895, and No. MRL88-19860.

[1] F. C. Frank, *Growth and Perfection of Crystals* (Wiley, New York, 1958).
[2] J. Villain, Nature (London) **350**, 273 (1991).
[3] O. Albrecht, H. Gruler, and E. J. Sackmann, J. Phys. (Paris) **39**, 301 (1978).
[4] C. M. Knobler, Science **249**, 870 (1990).
[5] H. Möhwald, Angew. Chem. Int. Ed. Engl. **27**, 728 (1988).
[6] H. M. McConnell, J. Phys. Chem. **94**, 4728 (1990).
[7] B. Berge, L. Faucheux, K. Schwab, and A. Libchaber, Nature (London) **350**, 322 (1991).
[8] See, for instance, F. Gallet, thesis, University of Paris, 1986 (unpublished).
[9] R. Perea-Carpio, F. Gonzalez-Caballero, J. M. Bruque, and G. Pardo, J. Colloid Interface Sci. **95**, 513–522 (1983).
[10] That is, a Ginzburg-Landau equation for a Lyapunov functional proportional to the length of the interface.
[11] J.-P. Eckmann, P. Meakin, I. Procaccia, and R. Zeitak, Phys. Rev. A **39**, 3185 (1989).

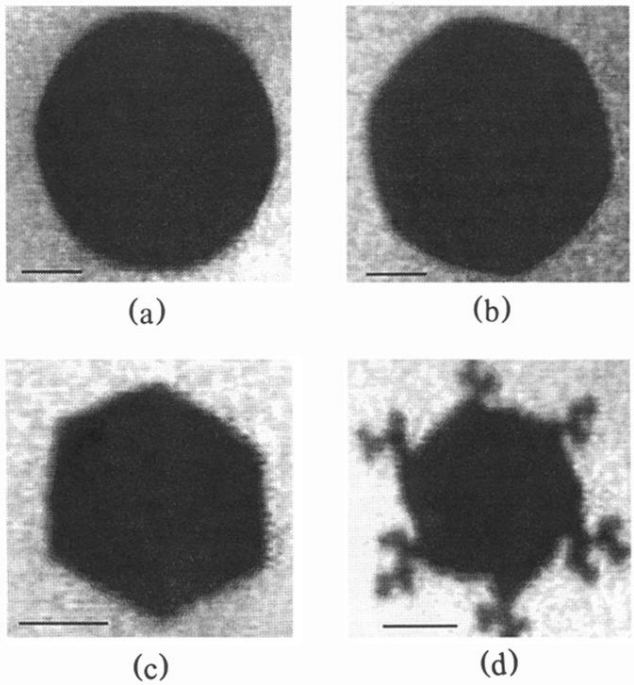

FIG. 1. Growth shapes for different cooling rates. (a) 0.1 mK/s; (b) 5 mK/s; (c) 50 mK/s; (d) 100 mK/s. Note the onset of destabilization into zigzags. Each bar is 10 μm long.

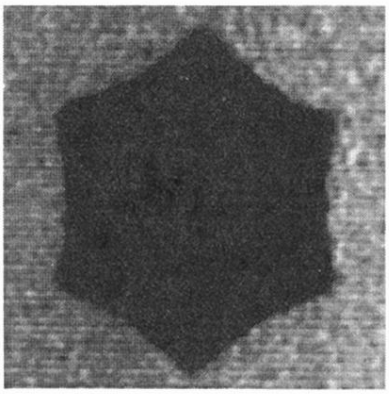

FIG. 3. Typical shape at the onset of destabilization. The waviness at the ridges of the star are due to discretization and imaging artifacts.